nature immunology

The MRE11-RAD50-NBS1 complex accelerates somatic hypermutation and gene conversion of immunoglobulin variable regions

Munehisa Yabuki, Monica M Fujii & Nancy Maizels

Targeted diversification of immunoglobulin variable regions is induced by activation-induced deaminase and may occur by either somatic hypermutation or gene conversion. MRE11-RAD50-NBS1 (MRN) is a ubiquitous and conserved nuclease complex critical for DNA break repair and is essential in class-switch recombination. Here we show that ectopic expression of NBS1, the regulatory subunit of MRN, accelerated hypermutation in the human B cell line Ramos and accelerated gene conversion in the chicken B cell line DT40. In both cases, accelerated diversification depended on MRN complex formation. These data suggest that MRN promotes DNA cleavage and/or mutagenic repair of lesions initiated by activation-induced deaminase, acting in the shared pathway of immunoglobulin gene diversification.

Somatic hypermutation, gene conversion and class-switch recombination alter the sequence and structure of immunoglobulin genes in B cells. Somatic hypermutation introduces nontemplated single-base changes into rearranged and expressed variable (V) regions; in humans and mice, this is coupled with selection to produce high-affinity antibodies. Gene conversion introduces tracts of mutations that are 'templated' by germline donor sequences; in chickens, this occurs before antigen stimulation to produce a diverse preimmune repertoire. Class-switch recombination joins a new constant region to a V region, carrying out region-specific DNA deletion that changes the mode of antigen clearance without altering antibody specificity.

All three processes of immunoglobulin gene diversification are initiated by the B cell–specific enzyme activation-induced deaminase (AID)[1–4], which deaminates C to U in transcribed single-stranded DNA[5–8]. Uracil in DNA can be faithfully repaired by a conserved pathway that depends on uracil-DNA glycosylase to remove uracil; apurinic-apyrimidinic endonuclease to cleave the phosphodiester backbone; and DNA polymerase-β and DNA ligase to repair the damage[9]. In B cells, the U produced after deamination by AID is removed by uracil-DNA glycosylase[10–13], but subsequent repair is mutagenic and leads to irreversible changes in genomic sequence and structure. The steps 'downstream' of AID and uracil-DNA glycosylase attack that lead to mutagenic repair have not been completely defined. Expression of AID is sufficient to activate hypermutation and class-switch recombination in non–B cells[14,15], so repair factors that act downstream of AID are ubiquitous and are not cell type specific.

MRE11-RAD50-NBS1 (MRN) is a ubiquitous and conserved nuclease complex involved in DNA break repair, cell cycle checkpoint control, meiotic recombination and telomere maintenance[16–18]. MRE11 and RAD50 are homologs of proteins first identified in yeast by their effects on meiotic recombination (MRE11) and radiation sensitivity (RAD50). NBS1 (also known as nibrin) is mutated in the human genetic disease Nijmegen breakage syndrome. MRE11 and RAD50 form the catalytic core of the MRN complex; exonucleolytic and endonucleolytic activities are vested in MRE11; and DNA binding and ATPase activities are in RAD50 (ref. 16). NBS1 is the regulatory subunit that interacts with MRE11 to govern nuclear localization and activities of the MRN complex[19–21]. NBS1 also responds to and regulates ATM kinase, which is missing in the human genetic disease ataxia-telangiectasia and is critical for cell cycle checkpoint signaling[22,23].

Participation of MRN in class-switch recombination has been demonstrated by several lines of experimentation. NBS1 localizes to switch regions in activated primary mouse B cells, and this localization is AID dependent[24]. Ablation of the gene encoding NBS1 is lethal in mice[25], but its function in class-switch recombination has been studied in conditional knockout mice, which show impaired class-switch recombination as well as pronounced genomic instability[26,27]. In the human genetic diseases Nijmegen breakage syndrome and ataxia-telangiectasia–like disorder, which result from hypomorphic mutations of NBS1 and MRE11, respectively, reduced titers of switched serum isotypes and altered switch junctions are evident[28–30]. Despite the facts that MRN is involved in DNA break repair and null mutations in any of the three genes encoding the MRN subunits are embryonically lethal in mice[25,31,32], no gross defect in DNA repair has been reported so far in Nijmegen breakage syndrome

Departments of Immunology and Biochemistry, University of Washington School of Medicine, Seattle, Washington 98195-7650, USA. Correspondence should be addressed to N.M. (maizels@u.washington.edu).

Published online 5 June 2005; doi:10.1038/ni1215

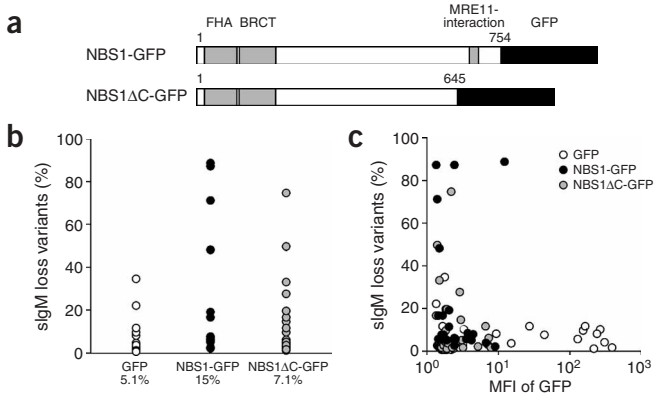

Figure 1 Increased NBS1 expression accelerates V-region diversification. (**a**) NBS1-GFP and NBS1ΔC-GFP constructs used for transfections. FHA, forkhead-associated domain; BRCT, BRCA1 carboxy-terminal domain. (**b**) The sIgM loss variants in Ramos GFP, NBS1-GFP and NBS1ΔC-GFP transfectants. Data represent the fraction of sIgM$^-$ cells in panels of individual clonal transfectants propagated for 4 weeks after transfection. Total number of individual transfectants analyzed and presented here: GFP, 45; NBS1-GFP, 19; NBS1ΔC-GFP, 37. Similar results were obtained in three independent transfection experiments. Below graph, mean sIgM loss frequencies from three experiments. (**c**) Mean fluorescence intensity (MFI) of GFP in independent Ramos GFP, NBS1-GFP and NBS1ΔC-GFP transfectants (horizontal axis) plotted relative to the fraction of sIgM loss variants in that culture (vertical axis) from data in **b**.

or ataxia-telangiectasia–like disorder cells[33,34]. This suggests that hypomorphic mutations may mask specific important functions of MRN.

The many critical functions of MRN limit genetic approaches to defining function of members of this complex *in vivo*. Nonetheless, repair and recombination factors are tightly regulated, and relatively small perturbations in their abundance or activity can have substantial effect on physiological processes. This has allowed testing of possible functions of the MRN complex in somatic hypermutation and gene conversion using an alternative strategy, which measures the effect of ectopic expression of the NBS1 regulatory subunit on somatic hypermutation and gene conversion. Here we report that ectopic NBS1 expression in either human or chicken B cell lines accelerated V-region diversification, causing increasing rates of nontemplated mutation in human B cells and templated mutation in chicken B cells. In human B cells transfected with NBS1, accelerated point mutation was accompanied by an increased fraction of mutations at C nucleotides and some DNA deletions. Acceleration of both hypermutation and gene conversion depended on the carboxy-terminal domain of NBS1, which interacts with MRE11 to form the MRN complex. This evidence for participation of the MRN nuclease complex in both nontemplated and templated diversification pathways, combined with evidence for involvement of MRN in class-switch recombination[24,26–30], leads us to propose that MRN can function in the shared pathway of B cell–specific immunoglobulin gene diversification, accelerating the processing of AID-initiated DNA lesions for subsequent mutagenic repair.

RESULTS

NBS1 accelerates hypermutation in human B cells

NBS1 is the regulatory subunit of the MRN complex, and it is necessary for transport of the MRE11-RAD50 heterotetramer from the cytoplasm to the nucleus[20,21]. To investigate the possible involvement of MRN in hypermutation, we generated stable transfectants of a surface immunoglobulin M–positive (sIgM$^+$) subclone of the constitutively hypermutating human B cell line Ramos with a plasmid expressing either green fluorescent protein (GFP) or a human NBS1–GFP fusion protein (**Fig. 1a**). This carboxy-terminal tag has been shown not to affect NBS1 function or localization[35]. We quantified V-region diversification using a standard sIgM loss assay, which measures accumulation of sIgM loss variants as a surrogate assay for hypermutation[36,37]. After 4 weeks of clonal expansion, the mean frequency of sIgM loss variants in the Ramos GFP control transfectants was 5.1% (**Fig. 1b**), almost identical to that of parental Ramos cells (4.0%; $n = 90$), whereas in the Ramos NBS1-GFP transfectants, the mean frequency was 15%, corresponding to a 2.9-fold stimulation of V-region diversification (**Fig. 1b**). This increase was comparable to the 2.8-fold increase in hypermutation rate noted after ectopic expression of an AID–GFP fusion protein in Ramos cells[38].

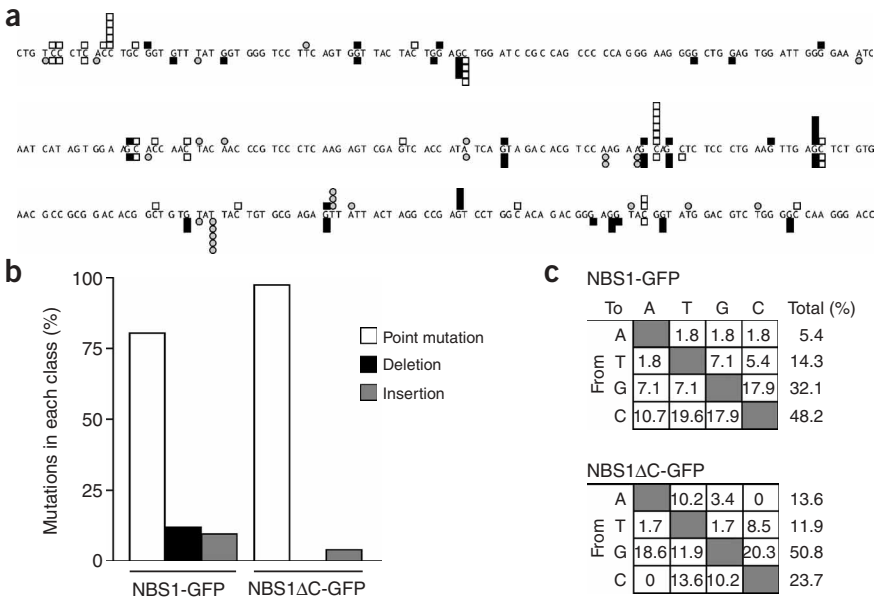

Figure 2 Distribution and spectra of mutations in Ramos cell V_H regions. (**a**) Point mutations in Ramos transfectants and sequence of the Ramos cell V_H region. Mutations in Ramos NBS1-GFP transfectants (above sequence) and Ramos NBS1ΔC-GFP transfectants (below sequence): open boxes, mutations at C; filled boxes, mutations at G; shaded circles, mutations at A and T. Number of symbols equals number of mutations at each position. (**b**) Distribution of classes of mutations (point mutations, deletions and insertions) in Ramos NBS1-GFP and NBS1ΔC-GFP transfectants. (**c**) Spectra of point mutations in Ramos NBS1-GFP and NBS1ΔC-GFP transfectants. Numbers indicate the percentage of each substitution in V_H regions.

MRN complex accelerates hypermutation

To determine if accelerated hypermutation was dependent on MRN complex formation, we measured the hypermutation rate in

Table 1 Mutation spectra in V_H regions of Ramos NBS1-GFP and NBS1ΔC-GFP transfectants

		Ramos NBS1-GFP	Ramos NBS1ΔC-GFP	Ramos[a]
Mutations at (%)	A	5.4	13.6	9.9
	T	14.3	11.9	8.1
	G	32.1	50.8	47.1
	C	48.2	23.7	34.8
	A + T	19.7	25.5	18.0
	G + C	80.3	74.5	81.9
Of mutations at G + C, fraction at (%)	G	40.0	68.2	57.5
	C	60.0	31.8	42.5
Transitions (%)		33.9	44.1	51.0
Transversions (%)		66.1	55.9	48.9

[a]Results for Ramos cells are from ref. 36.

Ramos derivatives expressing a truncated NBS1 mutant (NBS1ΔC-GFP; **Fig. 1a**) that lacks the carboxy-terminal domain necessary for interaction with MRE11 and MRN complex formation[20]. The mean frequency of sIgM loss variants in the Ramos NBS1ΔC-GFP transfectants was 7.1%, well below that of the Ramos NBS1-GFP transfectants and almost comparable to that of the Ramos GFP control transfectants (**Fig. 1b**). Accelerated hypermutation in Ramos NBS1 transfectants thus seemed to be due to increased amounts of the MRN complex.

Fluctuation analysis (**Fig. 1b**) showed considerable variation in the mutation rates of individual transfectant clones. Clonal history is one determinant of the fraction of sIgM loss variants in a culture, as mutations that occur early in a lineage will produce a higher fraction of sIgM loss variants than mutations that occur late[39]. In addition, differences in expression of NBS1-GFP or NBS1ΔC-GFP might contribute to variations in hypermutation rates among transfected clones. We assessed whether the abundance of NBS1-GFP or NBS1ΔC-GFP correlated with the hypermutation rate by quantifying ectopic expression of tagged protein in a panel of transfectants using flow cytometry. There was no correlation between hypermutation rate and NBS1-GFP or NBS1ΔC-GFP expression (**Fig. 1c**). Moreover, the green fluorescence signal was distinctly lower in Ramos NBS1-GFP and NBS1ΔC-GFP transfectants than in Ramos GFP control transfectants (**Fig. 1c**). Nuclear localization or sequestration of the tagged polypeptides in complexes of repair factors may have contributed to the relatively low intensity of the fluorescence signal. However, the magnitude of this difference and the fact that only very modest increases in ectopic expression were evident by immunoblot (data not shown) suggested that there may have been poor survival of clones with high expression of NBS1-GFP or NBS1ΔC-GFP.

NBS1 expression alters the hypermutation spectrum

Sequence analysis of the rearranged heavy-chain V (V_H) regions amplified from single cells from four independent Ramos NBS1-GFP transfectants showed that most mutations (80%) were point mutations (**Supplementary Fig. 1** online and **Fig. 2a**,**b**). Mutations were confined to the V_H regions, and we found no mutations in μ constant regions (of a total of 21,070 base pairs (bp) sequenced in 35 μ constant regions), as is typical of products of hypermutation in human B cells. The overall mutation frequency in Ramos NBS1-GFP transfectants was extremely high: we identified a total of 70 mutations in 96 V_H regions, whereas we found only 7 mutations in 96 V_H regions of the Ramos GFP control transfectants propagated in the same conditions. Of the point mutations in the Ramos NBS1-GFP transfectants, 80% were at C or G nucleotides ($P < 0.001$, χ^2 test; **Fig. 2c** and **Table 1**). Similarly, in Ramos cells[36], approximately 80% of mutations occurred at C or G nucleotides (**Table 1**). However, there was a distinct shift in the mutation spectrum in the Ramos NBS1-GFP transfectants. Notably, most mutations at C or G nucleotides were at C (60%), not G, distinct from what we noted for Ramos (43%; $P < 0.001$, χ^2 test; **Table 1**). In addition, the fraction of transversions was 66%, compared with 49% in Ramos cells ($P < 0.001$, χ^2 test; **Table 1**).

The V_H regions of the Ramos NBS1-GFP transfectants were further distinguished by deletion and insertion mutations (**Supplementary Fig. 1** online and **Fig. 2b**). Deletions and insertions were rarely present in Ramos cells[36] and the Ramos NBS1ΔC-GFP transfectants (**Fig. 2b**). Of the eight deletions identified in the Ramos NBS1-GFP transfectants, ranging in size from 1 to 124 bp (mean, 33 bp), all carried a C nucleotide at the 3′ endpoint, and in all deletions not accompanied by DNA insertion, the 5′ boundary was also a C nucleotide (**Supplementary Fig. 1** online). AID acts processively[40], and resection may have spanned the region between two C nucleotides deaminated by AID.

Sequence analysis of the rearranged V_H regions from 11 independent Ramos NBS1ΔC-GFP transfectants showed that most mutations (97%) were point mutations (**Supplementary Fig. 2** online and **Fig. 2a**). No deletions were evident and we identified only two insertions (**Supplementary Fig. 2** online and **Fig. 2b**). Of the point mutations, 75% were at C or G nucleotides ($P < 0.001$, χ^2 test; **Fig. 2c** and **Table 1**), comparable to those of the Ramos NBS1-GFP transfectants. A minority of mutations at C or G nucleotides were at C (32%), very different from the high fraction of mutations at C nucleotides in V_H regions from the Ramos NBS1-GFP transfectants (60%; $P < 0.001$, χ^2 test; **Table 1**). The fraction of transversions was 56%, lower than the 66% transversions found in the Ramos NBS1-GFP transfectants ($P < 0.05$, χ^2 test; **Table 1**).

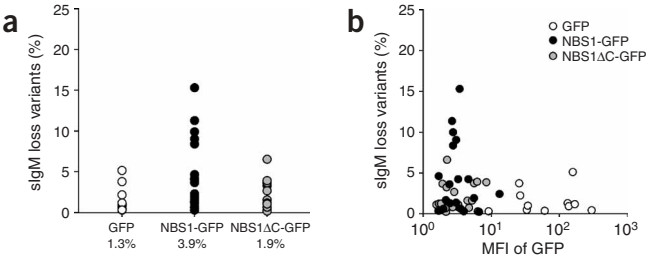

Figure 3 NBS1 expression accelerates gene conversion. (**a**) Fraction of sIgM loss variants in DT40 GFP, NBS1-GFP and NBS1ΔC-GFP transfectants. Variants were quantified after 6 weeks of clonal expansion. Total independently transfectant clones analyzed: GFP, 14; NBS1-GFP, 21; NBS1ΔC-GFP, 20. Similar results were obtained in four independent transfection experiments. Below graph, mean fraction of sIgM loss variants from four experiments. (**b**) Mean fluorescence intensity (MFI) of GFP in panels of independent DT40 GFP, NBS1-GFP and NBS1ΔC-GFP transfectants (horizontal axis) plotted relative to the fraction of sIgM loss variants (vertical axis) from data in **a**.

Table 2 Templated and nontemplated mutations and mutation frequencies in rearranged V_λ regions of DT40 transfectants

	DT40 NBS1-GFP	DT40 NBS1ΔC-GFP
DNA sequenced (bp)	41,140	30,624
Total mutations		
Templated	99	2
Nontemplated	10	2
Mutation frequency[a]		
Templated	2.4×10^{-3}	6.5×10^{-5}
Nontemplated	2.4×10^{-4}	6.5×10^{-5}

[a]Events per base pair.

Ectopic NBS1-GFP expression therefore both accelerated hypermutation and altered the spectrum of mutations, increasing the fraction of mutations at C nucleotides and the fraction of transversion mutations and also causing deletion and insertion mutations. Conversely, ectopic NBS1ΔC-GFP expression did not substantially accelerate hypermutation, but did cause a decrease in the fraction of mutations at C nucleotides.

MRN accelerates gene conversion in chicken B cells

To study the possible function of MRN in V-region diversification by gene conversion, we assayed the effect of ectopic expression of NBS1 on V-region mutation in the chicken bursal lymphoma line DT40. We generated stable transfectants of an $sIgM^+$ subclone of the DT40 line expressing either full-length NBS1 (NBS1-GFP) or the carboxy-terminal truncation mutant (NBS1ΔC-GFP). After 6 weeks of clonal expansion, the mean fraction of sIgM loss variants in DT40 GFP control transfectants was 1.3% (**Fig. 3a**). In DT40 NBS1-GFP transfectants, this fraction increased to 3.9% (**Fig. 3a**). The mean fraction of sIgM loss variants in the DT40 NBS1ΔC-GFP transfectants was 1.9%, comparable to that of the control transfectants (**Fig. 3a**). Thus, NBS1 accelerated V-region diversification threefold in chicken cells and the acceleration was dependent on MRN complex formation.

There was no direct correlation between frequency of sIgM loss and mean green fluorescence intensity in the DT40 NBS1-GFP and NBS1ΔC-GFP transfectants (**Fig. 3b**). This result was similar to results obtained with transfectants of the human B cell line Ramos (**Fig. 1c**). Moreover, green fluorescence intensities of DT40 NBS1-GFP and NBS1ΔC-GFP transfectants were considerably lower than those of DT40 GFP transfectants, suggesting that, as with Ramos, there may have been poor survival of clones with high expression of NBS1-GFP or NBS1ΔC-GFP.

To establish whether accelerated sIgM loss reflected an increase in gene conversion, we sequenced the rearranged λ light-chain V (V_λ) regions amplified from 110 single cells from 36 independent DT40 NBS1-GFP transfectants. Essentially all mutations (91%) were produced by gene conversion, as sequence changes could be assigned to donor tracts among the V_λ pseudogenes (**Supplementary Fig. 3** online and **Table 2**). The overall mutation frequency in the DT40 NBS1-GFP transfectants was 2.4×10^{-3} events per base pair (99 events per 41,140 bp sequenced), much higher than that in the DT40 NBS1ΔC-GFP transfectants (6.5×10^{-5} events per base pair; **Table 2**) or DT40 GFP control transfectants (not shown). Transfection with a plasmid expressing a full-length chicken NBS1-GFP had a similar effect on the gene conversion frequency (2.6×10^{-3} events per base pair). We found no mutations in unrearranged V_λ regions in DT40 NBS1-GFP transfectants (for a total of 10,700 bp sequenced in 20 V_λ regions). Thus, ectopic NBS1 expression accelerated V region diversification through gene conversion, the normal pathway of V gene diversification in chicken B cells.

Cell cycle is unaltered by NBS1 expression

The MRN complex responds to and regulates ATM kinase, which is involved in cell cycle checkpoint signaling[22,23]. To determine if the accelerated diversification caused by ectopic NBS1 expression reflected alterations in cell cycle progression, we analyzed the cell cycle distribution of representative Ramos and DT40 transfectants using propidium iodide staining. Cell cycle distribution was essentially identical in the Ramos (**Fig. 4a**) and DT40 (**Fig. 4b**) NBS1-GFP, NBS1ΔC-GFP and GFP transfectants. Therefore, it seems altered cell

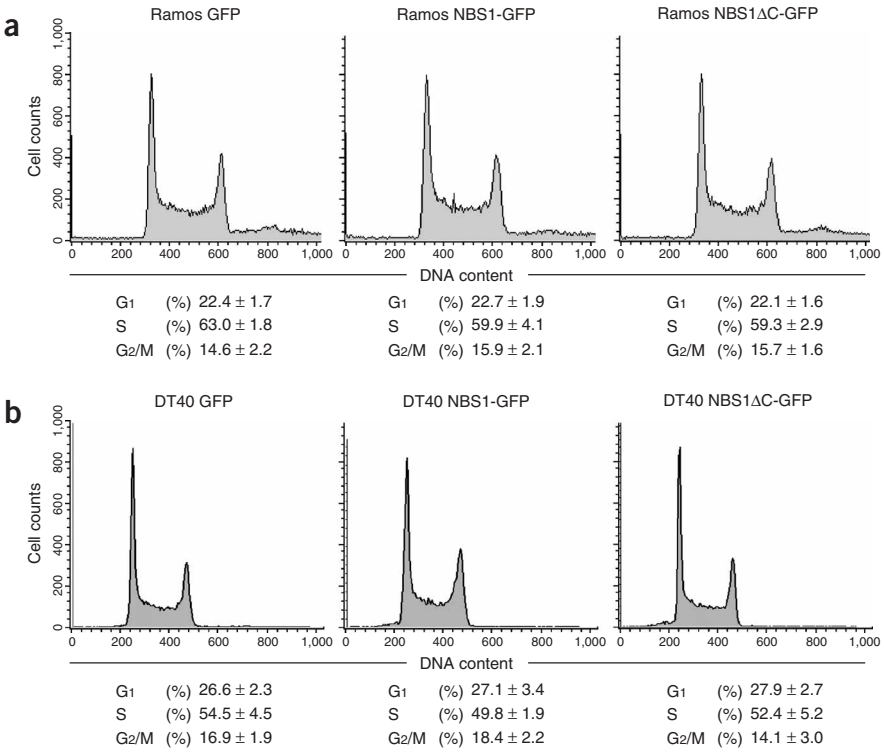

Figure 4 Cell cycle distribution is unaltered by NBS1 or NBS1ΔC expression. (**a**) Cell cycle distribution of Ramos GFP, NBS1-GFP and NBS1ΔC-GFP transfectants. Above, profiles of propidium iodide staining of representative clones; below, fractions of cells in G1, S and G2/M (mean ± s.d.) of five independent clones. (**b**) Cell cycle distribution of DT40 GFP, NBS1-GFP and NBS1ΔC-GFP transfectants. Data are presented as in **a**.

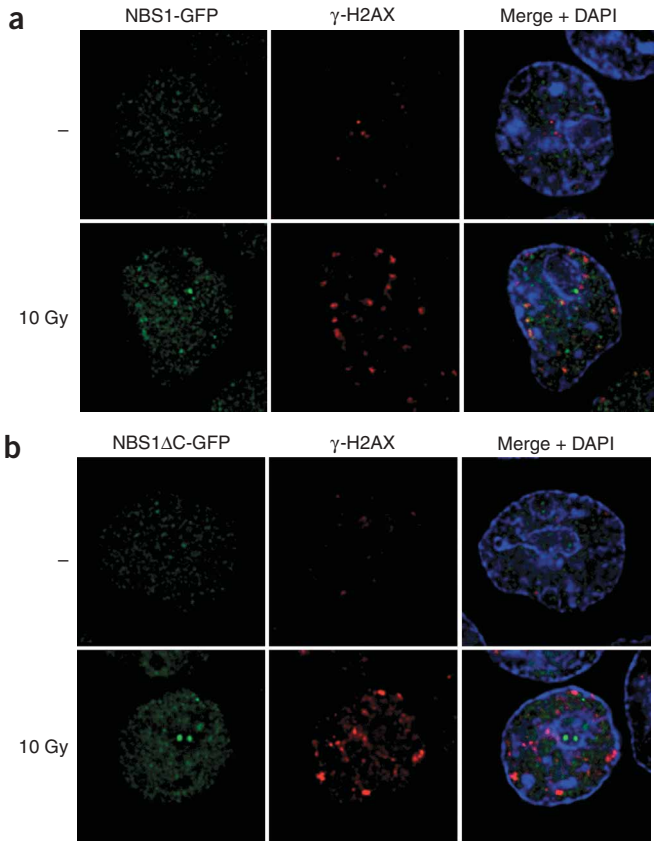

Figure 5 Ionizing radiation–induced focus formation by NBS1-GFP and NBS1ΔC–GFP. Immunofluorescence microscopy of representative transfectants analyzed before (–) or after (10 Gy) 10 Gy of ionizing radiation. (**a**) Ramos NBS1-GFP transfectants. (**b**) Ramos NBS1ΔC-GFP transfectants. Green, GFP-tagged protein; red, γ-H2AX; blue, 4,6-diamidino-2-phenylindole (DAPI). Merge, merged images from left and center panels. Similar results were obtained by analysis of DT40 cells.

cycle does not account for accelerated hypermutation or gene conversion induced by ectopic expression of NBS1.

NBS1ΔC does not stably associate with DNA damage

NBS1 interacts with MRE11-RAD50 nuclease for transport to the nucleus[20,21], but it is not known whether formation of the MRN complex is necessary for stable association of NBS1 with damaged DNA. We addressed this by comparing localization of either NBS1-GFP or NBS1ΔC-GFP with γ-H2AX, the phosphorylated histone variant generated at sites of ionizing radiation–induced DNA damage[41]. Deletion of the NBS1 carboxyl terminus impairs the function of NBS1 in the response to ionizing radiation, as the NBS1ΔC mutant cannot 'complement' the radiation sensitivity of cells from patients with Nijmegen breakage syndrome[20]. Immunofluorescence microscopy showed that NBS1-GFP localized to the nucleus in proliferating Ramos cells and, after irradiation, relocalized to foci that localized together with γ-H2AX (**Fig. 5a**), as reported before[35]. NBS1ΔC-GFP similarly localized to the nucleus in normally proliferating cells and formed foci after ionizing radiation; however, the ionizing radiation–induced NBS1ΔC-GFP foci were almost exclusively nucleolar and did not localize together with γ-H2AX (**Fig. 5b**). The simplest explanation for impaired localization of NBS1ΔC-GFP is that formation of the MRN complex is critical for stable association of NBS1 with sites of DNA damage, although we cannot rule out the possibility that this association is mediated indirectly through other factors that interact with the NBS1 carboxyl terminus. These results suggest that the ability of NBS1 but not NBS1ΔC to accelerate V-region diversification (**Figs. 1** and **3**) may reflect enhanced delivery of the MRN complex to AID-initiated lesions in the V regions and a resulting increase in the fraction of lesions that undergo mutagenic repair.

DISCUSSION

We have shown here that the MRN complex accelerates hypermutation in the human B cell line Ramos and gene conversion in the chicken B cell line DT40. In addition to the evidence that the MRN complex can participate in hypermutation and gene conversion, presented here, MRN has also been shown to have a key function in class-switch recombination[24,26–30]. Thus, MRN can act in the shared pathway of B cell–specific immunoglobulin gene diversification. Involvement of ubiquitous factors in this pathway was anticipated by experiments showing that AID is the only B cell–specific factor required for either somatic hypermutation or class-switch recombination[14,15].

Ectopic expression of NBS1 accelerated sIgM loss in human and chicken B cells 2.9-fold and 3-fold, respectively. This result is comparable to the 2.8-fold acceleration caused by ectopic expression of AID-GFP in human B cells[38]. These observations suggest that there may be physiological limitations on the rate of targeted immunoglobulin gene diversification in B cells. This pathway may be regulated by the activity or abundance of a single factor; it will be useful to determine if higher rates of diversification can be achieved by expression of both AID and NBS1 together. It is also possible that cells in which the 'ceiling' on the immunoglobulin diversification rate is exceeded may experience collateral damage to other gene that proves lethal. The fact that the GFP signals of NBS1-GFP and NBSΔC-GFP transfectants of Ramos and DT40 cells were lower than those of the GFP control transfectants suggests that large increases in NBS1 activity may be toxic in these AID-expressing B cells. It will be interesting to learn whether all cells are similarly sensitive to small perturbations in MRN abundance.

The molecular signatures of hypermutation and gene conversion are distinct[42]. Hypermutated human and mouse V regions contain almost exclusively single-base changes with no obvious matches in germline DNA[43]. In contrast, chicken V regions, which undergo targeted gene conversion, contain tracts of mutations with obvious templates in upstream 'pseudo-V' segments. The evidence that NBS1 expression accelerates both processes without altering the distinctive molecular signature indicates direct participation of MRN in both pathways.

The contrasting molecular signatures of hypermutation and gene conversion raise the issue of how a single factor might accelerate both. Alterations in the mutation spectra in Ramos NBS1-GFP transfectants provide insight into a possible mechanism. Somatic hypermutation occurs in at least two separable phases[43], distinguished by dependence on specific factors. Phase 1 produces transition mutations at C-G nucleotides, which are thought to arise when U-G mismatches undergo replicative repair[11,12]. Phase 2 depends on the mismatch repair factors MutSα (a heterodimer of MSH2 and MSH6) and EXO1 and creates mutations at A-T nucleotides[43]. MRN does not seem to contribute specifically to either phase 1 or phase 2 of hypermutation, as neither transition-biased mutations (phase 1) nor A-T–biased mutations (phase 2) were increased in Ramos NBS1-GFP transfectants. Instead, an increased fraction of transversion mutations was evident as a result of increased NBS1 expression. Conversely, in human genetic disease, hypomorphic mutations in *NBS1* cause a decrease in the fraction of transversion mutations[30].

Increased DNA breaks seem to result from NBS1 expression in both chicken and human B cells. Gene conversion requires a DNA break to produce a free 3′ end on which to prime templated DNA synthesis in the recipient gene, and the accelerated gene conversion documented in DT40 NBS1-GFP transfectants was probably due to increased DNA cleavage. A few nontemplated mutations accompanied gene conversion in the DT40 NBS1-GFP transfectants, and these mutations were almost exclusively (nine of ten mutations) at C-G nucleotides, suggesting involvement of MRN at sites of AID-initiated damage. As with gene conversion, deletion and insertion mutations originate with DNA breaks, and such mutations were evident in Ramos NBS1-GFP transfectants. These results suggest that MRN might stimulate either DNA cleavage at abasic sites or mutagenic repair of cleaved sites.

We therefore propose that MRN promotes DNA cleavage and/or mutagenic repair at AID-initiated lesions, functioning downstream of AID and uracil-DNA glycosylase. An increased rate of processing of AID-initiated lesions by either of these mechanisms would explain the observed acceleration of both hypermutation and gene conversion in NBS1 transfectants and the transversion-biased mutation spectrum. AID attacks C nucleotides, and MRN involvement in DNA cleavage or repair at the sites of AID attack would also account for the increased fraction of mutation at C nucleotides in Ramos NBS1-GFP transfectants and the fact that deletions in Ramos transfectants are in essentially all cases bounded by C nucleotides.

Involvement of MRN in DNA cleavage or break repair would be consistent with the function of MRN in class-switch recombination that has been documented previously[24,26–30]. In fact, the deletion and insertion mutations identified in V regions of Ramos NBS1-GFP transfectants resemble some products of class-switch recombination, particularly deletions within switch regions that can be a byproduct of productive recombination[44]. Deletions and insertions have also been documented in rearranged V regions of human germinal center B cells[45], suggesting that DNA breaks indeed accompany somatic hypermutation.

MRN may participate in the shared B cell–specific pathway of immunoglobulin gene diversification in several ways. It may bind to and stabilize AID-initiated lesions for repair, consistent with evidence that the carboxy-terminal region of NBS1 is required not only for acceleration of hypermutation and gene conversion but also for stable association with sites of DNA damage. MRN may also recruit other repair factors, similar to its proposed function as a sensor for genetic damage[17,18]. MRN may also function as a nuclease, participating directly in DNA cleavage, consistent with activities demonstrated *in vitro*[19,46,47]. Additional work is needed to determine the mechanistic details of the function of MRN at the immunoglobulin loci.

METHODS

Plasmid constructs. The human NBS1-GFP expression construct was a gift from P. Concannon (Benaroya Research Institute, Seattle, Washington). The NBS1ΔC derivative, which contains only residues 1–645, was amplified from this construct with the primers 5′-AGATCTCGAGCTCAAGCTTC-3′ and 5′-TAGGATCCTGAAGTTTGTCATTGTTAGATATTTC-3′ and was cloned into the GFP vector pEGFP-N1 (Clontech).

Cell culture and sIgM loss assay. The human Burkitt lymphoma line Ramos (RA1; purchased from American Type Culture Collection) was maintained at 37 °C in RPMI 1640 medium supplemented with 10% fetal calf serum, 50 μM 2-mercaptoethanol, 2 mM L-glutamine and antibiotics. The chicken bursal lymphoma line DT40 (CL18; provided by S. Takeda, Kyoto University, Kyoto, Japan) was maintained as described above, except that 1% chicken serum (Invitrogen) was also added to the medium.

Quantification of the fraction of $sIgM^-$ cells after a fixed period of culture was used as a convenient surrogate measure of the rate of V-region diversification. In B cells carrying out programmed V-region diversification, a substantial fraction of mutations impairs the expression of full-length heavy- or light-chain polypeptides or association of these polypeptides with each other. Such mutations result in loss of sIgM expression, which can be readily measured by staining with antibodies to IgM, followed by flow cytometry. For assay of sIgM loss, $sIgM^+$ subclones of Ramos and DT40 were isolated by limiting dilution and were transfected by electroporation and, after drug selection, individual clones were expanded (Ramos, 4 weeks; DT40, 6 weeks). The sIgM loss variants were quantified by flow cytometry as described[36,37]. Approximately 1×10^6 cells were stained with R-phycoerythrin–conjugated antibody to IgM (Southern Biotechnology Associates) and were analyzed on a FACScan with CellQuest software (Becton Dickinson). A total of 20,000 events or more were collected and dead cells were excluded by forward- and side-scatter gating.

Single-cell PCR and sequence analysis. Single cells were directly sorted into microplates containing 10 μl of PCR buffer, were stored at –20 °C until use and were then incubated for 1 h at 50 °C and 5 min at 95 °C with 250 μg/ml of proteinase K. The rearranged V_H region in Ramos was amplified by seminested PCR with high-fidelity PfuTurbo DNA polymerase (Stratagene), two first-round primers (5′-CCCCAAGCTTCCCAGGTGCAGCTACAGCAG-3′ and 5′-GCGGTACCTGAGGAGACGGTGACC-3′)[36] and an additional second-round primer (5′-ACCTGAGGAGACGGTGACCGTGGT-3′). The rearranged V_λ region in DT40 was also amplified by seminested PCR with two first-round primers (5′-CAGGAGCTCGCGGGGCCGTCACTGATTGCCG-3′ and 5′-GCG CAAGCTTCCCCAGCCTGCCGCCAAGTCCAAG-3′)[37] and a second-round primer (5′-TCACTGATTGCCGTTTTCTCCCCTCTCTCC-3′). PCR products were purified on Microcon (Millipore) and were sequenced directly. Mutations were identified by sequence alignment with MultAlin (http://prodes.toulouse.inra.fr/multalin/multalin.html). Potential gene conversion tracts in DT40 V_λ were identified by sequence comparison with the known V_λ pseudogene sequences[48,49]. The χ^2 test was used for evaluation of the statistical significance of differences observed.

Cell cycle analysis. Cells (about 5×10^6) from an exponentially growing culture were fixed in ethanol at 4 °C overnight, were treated at 37 °C for 30 min with 50 μg/ml of propidium iodide (Sigma) and 1 mg/ml of RNase A (Sigma) and were analyzed by flow cytometry with FlowJo software (Tree Star).

Immunofluorescence staining. Immunofluorescence staining was done as described[50] with a 1:500 dilution of a monoclonal antibody to γ-H2AX (Upstate). Captured fluorescent images were processed with a deconvolution algorithm to remove out-of-focus information.

Note: Supplementary information is available on the Nature Immunology website.

ACKNOWLEDGMENTS

We thank K. Utsumi; M. Bravo for assistance with cell sorting; G. Martin at the Keck Imaging Center (University of Washington, Seattle, Washington) for help with deconvolution microscopy; D. Bednarski, M. Huber and M. Weiner for help with DNA sequencing; A. Yabuki for assistance in preliminary experiments; and members of the Maizels laboratory for discussions. M.Y. was on leave from the Institute of Medical Science, Kurashiki Medical Center, Kurashiki 710-8522, Japan. Supported by the US National Institutes of Health (R01 GM39799 and R01 GM41712 to N.M.).

COMPETING INTERESTS STATEMENT

The authors declare that they have no competing financial interests.

Received 22 March; accepted 12 May 2005
Published online at http://www.nature.com/natureimmunology/

1. Muramatsu, M. *et al.* Class switch recombination and hypermutation require activation-induced cytidine deaminase (AID), a potential RNA editing enzyme. *Cell* **102**, 553–563 (2000).
2. Revy, P. *et al.* Activation-induced cytidine deaminase (AID) deficiency causes the autosomal recessive form of the hyper-IgM syndrome (HIGM2). *Cell* **102**, 565–575 (2000).

3. Arakawa, H., Hauschild, J. & Buerstedde, J.M. Requirement of the activation-induced deaminase (AID) gene for immunoglobulin gene conversion. *Science* **295**, 1301–1306 (2002).
4. Harris, R.S., Sale, J.E., Petersen-Mahrt, S.K. & Neuberger, M.S. AID is essential for immunoglobulin V gene conversion in a cultured B cell line. *Curr. Biol.* **12**, 435–438 (2002).
5. Petersen-Mahrt, S.K., Harris, R.S. & Neuberger, M.S. AID mutates *E. coli* suggesting a DNA deamination mechanism for antibody diversification. *Nature* **418**, 99–104 (2002).
6. Bransteitter, R., Pham, P., Scharff, M.D. & Goodman, M.F. Activation-induced cytidine deaminase deaminates deoxycytidine on single-stranded DNA but requires the action of RNase. *Proc. Natl. Acad. Sci. USA* **100**, 4102–4107 (2003).
7. Chaudhuri, J. *et al.* Transcription-targeted DNA deamination by the AID antibody diversification enzyme. *Nature* **422**, 726–730 (2003).
8. Ramiro, A.R., Stavropoulos, P., Jankovic, M. & Nussenzweig, M.C. Transcription enhances AID-mediated cytidine deamination by exposing single-stranded DNA on the nontemplate strand. *Nat. Immunol.* **4**, 452–456 (2003).
9. Barnes, D.E. & Lindahl, T. Repair and genetic consequences of endogenous DNA base damage in mammalian cells. *Annu. Rev. Genet.* **38**, 445–476 (2004).
10. Di Noia, J. & Neuberger, M.S. Altering the pathway of immunoglobulin hypermutation by inhibiting uracil-DNA glycosylase. *Nature* **419**, 43–48 (2002).
11. Rada, C. *et al.* Immunoglobuin isotype switching is inhibited and somatic hypermutation perturbed in UNG-deficient mice. *Curr. Biol.* **12**, 1748–1755 (2002).
12. Imai, K. *et al.* Human uracil-DNA glycosylase deficiency associated with profoundly impaired immunoglobulin class-switch recombination. *Nat. Immunol.* **4**, 1023–1028 (2003).
13. Di Noia, J.M. & Neuberger, M.S. Immunoglobulin gene conversion in chicken DT40 cells largely proceeds through an abasic site intermediate generated by excision of the uracil produced by AID-mediated deoxycytidine deamination. *Eur. J. Immunol.* **34**, 504–508 (2004).
14. Yoshikawa, K. *et al.* AID enzyme-induced hypermutation in an actively transcribed gene in fibroblasts. *Science* **296**, 2033–2036 (2002).
15. Okazaki, I.M., Kinoshita, K., Muramatsu, M., Yoshikawa, K. & Honjo, T. The AID enzyme induces class switch recombination in fibroblasts. *Nature* **416**, 340–345 (2002).
16. D'Amours, D. & Jackson, S.P. The Mre11 complex: at the crossroads of DNA repair and checkpoint signalling. *Nat. Rev. Mol. Cell Biol.* **3**, 317–327 (2002).
17. Petrini, J.H. & Stracker, T.H. The cellular response to DNA double-strand breaks: defining the sensors and mediators. *Trends Cell Biol.* **13**, 458–462 (2003).
18. van den Bosch, M., Bree, R.T. & Lowndes, N.F. The MRN complex: coordinating and mediating the response to broken chromosomes. *EMBO Rep.* **4**, 844–849 (2003).
19. Paull, T.T. & Gellert, M. Nbs1 potentiates ATP-driven DNA unwinding and endonuclease cleavage by the Mre11/Rad50 complex. *Genes Dev.* **13**, 1276–1288 (1999).
20. Desai-Mehta, A., Cerosaletti, K.M. & Concannon, P. Distinct functional domains of nibrin mediate Mre11 binding, focus formation, and nuclear localization. *Mol. Cell. Biol.* **21**, 2184–2191 (2001).
21. Tauchi, H. *et al.* The forkhead-associated domain of NBS1 is essential for nuclear foci formation after irradiation but not essential for hRAD50·hMRE11·NBS1 complex DNA repair activity. *J. Biol. Chem.* **276**, 12–15 (2001).
22. Stracker, T.H., Theunissen, J.W., Morales, M. & Petrini, J.H. The Mre11 complex and the metabolism of chromosome breaks: the importance of communicating and holding things together. *DNA Repair (Amst.)* **3**, 845–854 (2004).
23. Bartek, J., Lukas, C. & Lukas, J. Checking on DNA damage in S phase. *Nat. Rev. Mol. Cell Biol.* **5**, 792–804 (2004).
24. Petersen, S. *et al.* AID is required to initiate Nbs1/γ-H2AX focus formation and mutations at sites of class switching. *Nature* **414**, 660–665 (2001).
25. Zhu, J., Petersen, S., Tessarollo, L. & Nussenzweig, A. Targeted disruption of the Nijmegen breakage syndrome gene NBS1 leads to early embryonic lethality in mice. *Curr. Biol.* **11**, 105–109 (2001).
26. Kracker, S. *et al.* Nibrin functions in Ig class-switch recombination. *Proc. Natl. Acad. Sci. USA* **102**, 1584–1589 (2005).
27. Reina-San-Martin, B., Nussenzweig, M.C., Nussenzweig, A. & Difilippantonio, S. Genomic instability, endoreduplication, and diminished Ig class-switch recombination in B cells lacking Nbs1. *Proc. Natl. Acad. Sci. USA* **102**, 1590–1595 (2005).
28. Pan, Q. *et al.* Alternative end joining during switch recombination in patients with ataxia-telangiectasia. *Eur. J. Immunol.* **32**, 1300–1308 (2002).
29. Pan-Hammarstrom, Q. *et al.* ATM is not required in somatic hypermutation of VH, but is involved in the introduction of mutations in the switch μ region. *J. Immunol.* **170**, 3707–3716 (2003).
30. Lahdesmaki, A., Taylor, A.M., Chrzanowska, K.H. & Pan-Hammarstrom, Q. Delineation of the role of the Mre11 complex in class switch recombination. *J. Biol. Chem.* **279**, 16479–16487 (2004).
31. Xiao, Y. & Weaver, D.T. Conditional gene targeted deletion by Cre recombinase demonstrates the requirement for the double-strand break repair Mre11 protein in murine embryonic stem cells. *Nucleic Acids Res.* **25**, 2985–2991 (1997).
32. Luo, G. *et al.* Disruption of mRad50 causes embryonic stem cell lethality, abnormal embryonic development, and sensitivity to ionizing radiation. *Proc. Natl. Acad. Sci. USA* **96**, 7376–7381 (1999).
33. Nove, J., Little, J.B., Mayer, P.J., Troilo, P. & Nichols, W.W. Hypersensitivity of cells from a new chromosomal-breakage syndrome to DNA-damaging agents. *Mutat. Res.* **163**, 255–262 (1986).
34. Stewart, G.S. *et al.* The DNA double-strand break repair gene hMRE11 is mutated in individuals with an ataxia-telangiectasia-like disorder. *Cell* **99**, 577–587 (1999).
35. Lukas, C., Falck, J., Bartkova, J., Bartek, J. & Lukas, J. Distinct spatiotemporal dynamics of mammalian checkpoint regulators induced by DNA damage. *Nat. Cell Biol.* **5**, 255–260 (2003).
36. Sale, J.E. & Neuberger, M.S. TdT-accessible breaks are scattered over the immunoglobulin V domain in a constitutively hypermutating B cell line. *Immunity* **9**, 859–869 (1998).
37. Sale, J.E., Calandrini, D.M., Takata, M., Takeda, S. & Neuberger, M.S. Ablation of XRCC2/3 transforms immunoglobulin V gene conversion into somatic hypermutation. *Nature* **412**, 921–926 (2001).
38. Rada, C., Jarvis, J.M. & Milstein, C. AID-GFP chimeric protein increases hypermutation of Ig genes with no evidence of nuclear localization. *Proc. Natl. Acad. Sci. USA* **99**, 7003–7008 (2002).
39. Luria, S.E. & Delbrück, M. Mutations of bacteria from virus sensitivity to virus resistance. *Genetics* **28**, 491–511 (1943).
40. Pham, P., Bransteitter, R., Petruska, J. & Goodman, M.F. Processive AID-catalysed cytosine deamination on single-stranded DNA simulates somatic hypermutation. *Nature* **424**, 103–107 (2003).
41. Rogakou, E.P., Pilch, D.R., Orr, A.H., Ivanova, V.S. & Bonner, W.M. DNA double-stranded breaks induce histone H2AX phosphorylation on serine 139. *J. Biol. Chem.* **273**, 5858–5868 (1998).
42. Maizels, N. Immunoglobulin gene diversification *Annu. Rev. Genetics* (in the press).
43. Neuberger, M.S. *et al.* Somatic hypermutation at A.T pairs: polymerase error versus dUTP incorporation. *Nat. Rev. Immunol.* **5**, 171–178 (2005).
44. Dudley, D.D. *et al.* Internal IgH class switch region deletions are position-independent and enhanced by AID expression. *Proc. Natl. Acad. Sci. USA* **99**, 9984–9989 (2002).
45. Goossens, T., Klein, U. & Kuppers, R. Frequent occurrence of deletions and duplications during somatic hypermutation: implications for oncogene translocations and heavy chain disease. *Proc. Natl. Acad. Sci. USA* **95**, 2463–2468 (1998).
46. Paull, T.T. & Gellert, M. The 3′ to 5′ exonuclease activity of Mre 11 facilitates repair of DNA double-strand breaks. *Mol. Cell* **1**, 969–979 (1998).
47. Trujillo, K.M., Yuan, S.S., Lee, E.Y. & Sung, P. Nuclease activities in a complex of human recombination and DNA repair factors Rad50, Mre11, and p95. *J. Biol. Chem.* **273**, 21447–21450 (1998).
48. Reynaud, C.A., Anquez, V., Grimal, H. & Weill, J.C. A hyperconversion mechanism generates the chicken light chain preimmune repertoire. *Cell* **48**, 379–388 (1987).
49. McCormack, W.T., Hurley, E.A. & Thompson, C.B. Germ line maintenance of the pseudogene donor pool for somatic immunoglobulin gene conversion in chickens. *Mol. Cell. Biol.* **13**, 821–830 (1993).
50. Liu, Y., Li, M-J., Lee, E.Y-H.P. & Maizels, N. Localization and dynamic relocalization of mammalian Rad52 during the cell cycle and in response to DNA damage. *Curr. Biol.* **9**, 975–978 (1999).